Structural Engineering and Mechanics, *Vol. 82, No. 6 (2022) 725-734*
https://doi.org/10.12989/sem.2022.82.6.725

Flexural and free vibration responses of thick isotropic bridge deck using a novel two variable refined plate theory

Fatima Zohra Djidar[1], Habib Hebali[2,3], Khaled Amara*[4], Abdelouahed Tounsi[2,5,6,7], Boudjema Bendaho[2], M.H. Ghazwani[8] and Muzamal Hussain[9]

[1]*Smart Structures Laboratory, University of Ain Témouchent, Faculty of Science & Technology, Civil Engineering Department, Algeria*
[2]*Material and Hydrology Laboratory, Civil Engineering Department, Faculty of Technology, University of Sidi Bel Abbes, Algeria*
[3]*Civil Engineering Department, Faculty of Science & Technology, University of Mascara, Algeria*
[4]*Engineering and Sustainable Development Laboratory, University of Ain Temouchent, Ain Temouchent 46000, Algeria*
[5]*YFL (Yonsei Frontier Lab), Yonsei University, Seoul, Korea*
[6]*Department of Civil and Environmental Engineering, King Fahd University of Petroleum & Minerals, 31261 Dhahran, Eastern Province, Saudi Arabia*
[7]*Interdisciplinary Research Center for Construction and Building Materials, KFUPM, 31261 Dhahran, Saudi Arabia*
[8]*Department of Mechanical Engineering, Faculty of Engineering, Jazan University, P.O Box 45124, Jazan, Kingdom of Saudia Arabia*
[9]*Department of Mathematics, Govt. College University Faisalabad, 38000, Faisalabad, Pakistan*

(*Received March 25, 2021, Revised March 12, 2022, Accepted March 24, 2022*)

Abstract. This work presents a simple exponential shear deformation theory for the flexural and free vibration responses of thick bridge deck. Contrary to the existing higher order shear deformation theories (HSDT) and the first shear deformation theory (FSDT), the proposed model uses a new displacement field which incorporates undetermined integral terms and involves only two variables. Governing equations and boundary conditions of the theory are derived by the principle of virtual work. The simply supported thick isotropic square and rectangular plates are considered for the detailed numerical studies. Results of displacements, stresses and frequencies are compared with those of other refined theories and exact theory to show the efficiency of the proposed theory. Good agreement is achieved of the present results with those of higher order shear deformation theory (HSDT) and elasticity theory. Moreover, results demonstrate that the developed two variable refined plate theory is simple for solving the flexural and free vibration responses of thick bridge deck and can achieve the same accuracy of the existing HSDTs which have more number of variables.

Keywords: free vibration; isotropic plates; refined plate theory; static flexure; transverse shear stresses

1. Introduction

Plates are vastly used in industry and new fields of technology such as aeronautical, marine, civil and mechanical engineering. The transverse shear and transverse normal deformation effects are definite in shear flexible plates which may be made up of isotropic, orthotropic, anisotropic or laminated composite materials. In company with investigations of stability response of plate, a great number of plate models have been proposed.

The simplest one is the classical plate theory (CPT), which ignores the transverse shear influences, provides reasonable results for thin and isotropic plates. In order to overcome the limitations of CPT, the shear deformation theories accounted for the effect of transverse shear deformation have been recommended. The first-order shear deformation theory (FSDT) assumes linear variation of in-planed in placements through the thickness. The FSDT which is known as the Reissner (1945) and Mindlin (1951) and consider the transverse shear influences by the way of linear distribution of the displacements across the thickness. In this theory, the relation between the resultant shear forces and the shear strains depends on shear correction factors. Many investigations have been presented in different scientific articles by employing FSDT for the free vibration

behavior of composite plates (Yan *et al*. 1966, Whitney 1969, Whitney and Pagano 1970, Ambartsumyan 1970, Sun and Whitney 1973, Bert and Chen 1978, Reddy 1979, Kant and Swaminathan 2001). Some other plate theories, e.g., higher-order shear deformation theories (HSDT), which include the effect of transverse shear strains, are reported in the literature. Reddy (1984) has put forward a modified third-order theory which considers not only the transverse shear strains, but also their parabolic variation across the plate thickness. As a result, there is no need to use shear correction coefficients in computing the shear stresses. Touratier *et al*. (1991) has used trigonometric functions for describing the parabolic distribution of transverse shear strains across the plate thickness. Mantari and Granados (2015) proposed a new FSDT with four variables in which integral terms in the plate kinematics are utilized. Since FSDTs do not respect equilibrium conditions at the top and bottom surfaces of the plate, shear correction coefficients are needed to correct the unrealistic distribution of the shear strain/stress within the thickness. For these reasons, many

*Corresponding author, Professor
E-mail: amara3176@yahoo.fr

ISSN: 1225-4568 (Print), 1598-6217 (Online)

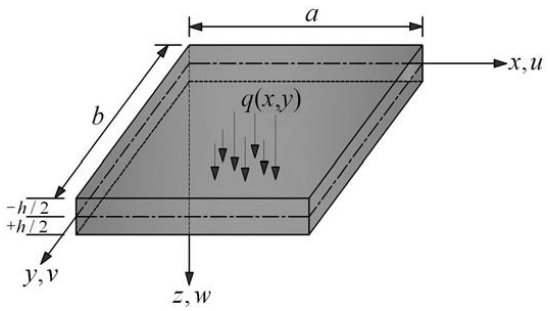

Fig. 1 Plate geometry and co-ordinate system

studies have used HSDTs to improve the limitations of FSDT such as Shahrjerdi *et al*. (2011), Viswanathan *et al*. (2013), Swaminathan and Naveenkumar (2014), Avcar (2019), Madenci (2019), Zouatnia and Hadji (2019) and Boulal *et al* (2020). Some studies on the mechanical characteristics of composite plate structure can be given by Ghodrati *et al*. (2017), Ton-That (2020), Pinto *et al* (2020), Koochi and Goharimanesh (2021). Recently, more attention has been paid to Artificial Neural Network using Arithmetic Optimization Algorithm for damage assessment in functionally graded material (FGM) plate structures such as Khatir *et al*. (2019), Zenzen *et al*. (2020), Tran-Ngoc *et al*. (2020), Khatir *et al*. (2021).

A three-dimensional (3D) solution for free vibration and buckling of annular plate, conical, cylinder and cylindrical shell of FG porous-cellular materials using Isogeometric analysis is presented by Cuong-Le *et al*. (2021). Damage detection on rectangular laminated composite plates using wavelet based Convolutional Neural Network Technique by Saadatmorad *et al*. (2021).

This paper presents the flexural and free vibration behaviors of thick isotropic bridge deck using a simple HSDT with two variables in which instead of derivative terms in the displacement field, integral terms are employed. The equations of motion are derived using Hamilton's principle. The fundamental frequencies are found by solving an eigenvalue equation. The results obtained by the present method are compared with solutions derived from other models known from the literature and are found to be in good agreement with them.

2. Theoretical formulation

2.1 Plate under consideration

Consider a plate (of length a, width b, and thickness h) made up of homogenous material. The plate occupies (in O-x-y-z right-handed Cartesian coordinate system) a region:

$0 \le x \le a\,; \qquad 0 \le y \le b\,; \qquad -h/2 \le z \le h/2$

2.2 Kinematics and strains

The field of displacement of the present model is expressed by the following relation

$$u(x,y,z,t) = -z\frac{\partial w_0}{\partial x} + K_1 f(z)\int \theta(x,y,t)\,dx \qquad (1a)$$

$$v(x,y,z,t) = -z\frac{\partial w_0}{\partial y} + K_2 f(z)\int \theta(x,y,t)\,dy \qquad (1b)$$

$$w(x,y,z,t) = w_0(x,y,t) \qquad (1c)$$

In this work, the present higher-order shear deformation plate theory is obtained by setting

$$f(z) = z\exp\left[-2\left(\frac{z}{h}\right)^2\right] \qquad (2)$$

The coefficients k_1 and k_2 depends on the geometry. It can be seen that the kinematic in Eq. (1) introduces only two unknowns (w_0 and θ).

The strain-displacement relations of the present theory can be obtained as follows

$$\begin{Bmatrix}\varepsilon_x\\ \varepsilon_y\\ \gamma_{xy}\end{Bmatrix} = z\begin{Bmatrix}k_x^b\\ k_y^b\\ k_{xy}^b\end{Bmatrix} + f(z)\begin{Bmatrix}k_x^s\\ k_y^s\\ k_{xy}^s\end{Bmatrix}, \begin{Bmatrix}\gamma_{yz}\\ \gamma_{xz}\end{Bmatrix} = g(z)\begin{Bmatrix}\gamma_{yz}^0\\ \gamma_{xz}^0\end{Bmatrix} \qquad (3)$$

where

$$\begin{Bmatrix}k_x^b\\ k_y^b\\ k_{xy}^b\end{Bmatrix} = \begin{Bmatrix}-\dfrac{\partial^2 w_0}{\partial x^2}\\ -\dfrac{\partial^2 w_0}{\partial y^2}\\ -\dfrac{\partial^2 w_0}{\partial x\partial y}\end{Bmatrix},$$

$$\begin{Bmatrix}k_x^s\\ k_y^s\\ k_{xy}^s\end{Bmatrix} = \begin{Bmatrix}k_1\theta\\ k_2\theta\\ k_1\dfrac{\partial}{\partial y}\int \theta\,dx + k_2\dfrac{\partial}{\partial x}\int \theta\,dy\end{Bmatrix}, \qquad (4a)$$

$$\begin{Bmatrix}\gamma_{yz}^0\\ \gamma_{xz}^0\end{Bmatrix} = \begin{Bmatrix}k_2\int \theta\,dy\\ k_1\int \theta\,dx\end{Bmatrix}$$

$$g(z) = \frac{df(z)}{dz} \qquad (4b)$$

The integrals used in the proposed kinematics must be determined by Navier's solution and can be given as follows

$$\frac{\partial}{\partial y}\int \theta\,dx = \acute{A}\frac{\partial^2\theta}{\partial x\partial y}, \frac{\partial}{\partial x}\int \theta\,dy = \acute{B}\frac{\partial^2\theta}{\partial x\partial y},$$
$$\int \theta\,dx = \acute{A}\frac{\partial\theta}{\partial x}, \int \theta\,dy = \acute{B}\frac{\partial\theta}{\partial y} \qquad (5)$$

In Eq. (5), the coefficients A' and B' are considered according to the type of solution used, in this case via Navier. Therefore, A', B', k_1 and k_2 are expressed as follows

$$\acute{A} = -\frac{1}{\lambda^2}, \acute{B} = -\frac{1}{\mu^2}, k_1 = \lambda^2, k_2 = \mu^2 \qquad (6)$$

where λ and μ are defined in expression (24).

For elastic and isotropic plate, the stress-strain relations can be expressed as follows

$$\begin{Bmatrix}\sigma_x\\ \sigma_y\\ \tau_{xy}\\ \tau_{yz}\\ \tau_{xz}\end{Bmatrix}=\begin{bmatrix}C_{11} & C_{12} & 0 & 0 & 0\\ C_{12} & C_{22} & 0 & 0 & 0\\ 0 & 0 & C_{66} & 0 & 0\\ 0 & 0 & 0 & C_{44} & 0\\ 0 & 0 & 0 & 0 & C_{55}\end{bmatrix}\begin{Bmatrix}\varepsilon_x\\ \varepsilon_y\\ \gamma_{xy}\\ \gamma_{yz}\\ \gamma_{xz}\end{Bmatrix} \tag{7}$$

where 'σ, τ' and 'ε, γ' are stresses and strains.

The elastics stiffness's C_{ij}, can be given as

$$C_{11}=C_{22}=\frac{E}{1-\nu^2}\,,C_{12}=\frac{\nu E}{1-\nu^2}\,,\quad C_{44}=C_{55}=C_{66}=\frac{E}{2(1+\nu)} \tag{8}$$

where E is the Young modulus and ν is the Poisons ration

2.3 Equations of motion

The Hamilton principle is used to determine the equations of motion

$$0=\int_0^t(\delta U+\delta V-\delta K)dt \tag{9}$$

where δU is the variation of strain energy; δV is the variation of potential energy; and δK is the variation of kinetic energy.

The variation of the strain energy of the isotropic plate is expressed as

$$\begin{aligned}\delta U&=\int_V\left[\sigma_x\delta\varepsilon_x+\sigma_y\delta\varepsilon_y+\tau_{xy}\delta\gamma_{xy}+\tau_{yz}\delta\gamma_{yz}+\tau_{xz}\delta\gamma_{xz}\right]dV\\&=\int_A\left[M_x\delta k_x^b+M_y\delta k_y^b+M_{xy}\delta k_{xy}^b+N_{sx}\delta k_x^s+N_{sy}\delta k_y^s+N_{sxy}\delta k_{xy}^s+N_{Tcx}\delta\gamma_{xz}^0+N_{Tcy}\delta\gamma_{yz}^0\right]dV\end{aligned} \tag{10}$$

where $\boldsymbol{A}$ is the top surface and the stress resultants $\boldsymbol{N}$, $\boldsymbol{M}$ are given by

$$\begin{aligned}\left(M_x,M_y,M_{xy}\right)&=\int_{-h/2}^{h/2}\left(\sigma_x,\sigma_y,\tau_{xy}\right)zdz\ ,\\\left(N_{sx},N_{sy},N_{sxy}\right)&=\int_{-h/2}^{h/2}\left(\sigma_x,\sigma_y,\tau_{xy}\right)f(z)dz\\\left(N_{Tcx},N_{Tcy},\right)&=\int_{-h/2}^{h/2}\left(\tau_{xz},\tau_{yz}\right)g(z)dz\end{aligned} \tag{11}$$

The variation in external work can be expressed as

$$\delta V=-\int_A q(x,y)\delta w_0dA \tag{12}$$

where $q(x,y)$ is transversal mechanical load

The variation of kinetic energy of the plate can be expressed as

$$\begin{aligned}\delta K&=\int_V\left(\ddot{u}\,\delta u+\ddot{v}\,\delta v+\ddot{w}\,\delta w\right)\rho dV\\&=\int_A\left\{I_1\ddot{w}_0\partial\ddot{w}_0+I_2\left(\frac{\partial\ddot{w}_0}{\partial x}\frac{\partial\delta w_0}{\partial x}+\frac{\partial\ddot{w}_0}{\partial y}\frac{\partial\delta w_0}{\partial y}\right)-I_3\left(K_1\acute{A}\frac{\partial\ddot{w}_0}{\partial x}\frac{\partial\delta\theta}{\partial x}+K_1\acute{A}\frac{\partial\ddot{\theta}}{\partial x}\frac{\partial\delta w_0}{\partial x}+K_2\acute{B}\frac{\partial\ddot{w}_0}{\partial y}\frac{\partial\delta\theta}{\partial y}+K_2\acute{B}\frac{\partial\ddot{\theta}}{\partial y}\frac{\partial\delta w_0}{\partial y}\right)+I_4\left(\left(K_1\acute{A}\right)^2\frac{\partial\ddot{\theta}}{\partial x}\frac{\partial\delta\theta}{\partial x}+\left(K_2\acute{B}\right)^2\frac{\partial\ddot{\theta}}{\partial y}\frac{\partial\delta\theta}{\partial y}\right)\right\}dA\end{aligned} \tag{13}$$

where dot-superscript convention indicates the differentiation with respect to the time variable t; ρ is the mass density; and I_i are mass inertias expressed by

$$\left(I_1,I_2,I_3,I_4\right)=\int_{-h/2}^{h/2}(1,z^2,zf(z),f(z)^2)\rho dz \tag{14}$$

By substituting Eqs. (10), (12) and (13) into Eq. (9), the equations of motion can be derived as follows:

$$\begin{aligned}&\delta w_0:-\frac{\partial^2M_x}{\partial x^2}-\frac{\partial^2M_y}{\partial y^2}-2\frac{\partial^2M_{xy}}{\partial x\partial y}-q=-I_1\frac{\partial^2w_0}{\partial t^2}+I_2\left(\frac{\partial^4w_0}{\partial x^2\partial t^2}+\frac{\partial^4w_0}{\partial y^2\partial t^2}\right)-I_3\left(K_1\acute{A}\frac{\partial^4\theta}{\partial x^2\partial t^2}+K_2\acute{B}\frac{\partial^4\theta}{\partial y^2\partial t^2}\right)\\&\delta\theta:K_1\acute{A}\frac{\partial^2N_{sx}}{\partial x^2}+K_2\acute{B}\frac{\partial^2N_{sy}}{\partial y^2}+\left(K_1\acute{A}+K_2\acute{B}\right)\frac{\partial^2N_{sxy}}{\partial x\partial y}-K_1\acute{A}\frac{\partial N_{Tcx}}{\partial x}-K_2\acute{B}\frac{\partial N_{Tcy}}{\partial y}=-I_3\left(K_1\acute{A}\frac{\partial^4w_0}{\partial x^2\partial t^2}+K_2\acute{B}\frac{\partial^4w_0}{\partial y^2\partial t^2}\right)+I_4\left(\left(K_1\acute{A}\right)^2\frac{\partial^4\theta}{\partial x^2\partial t^2}+\left(K_2\acute{B}\right)^2\frac{\partial^4\theta}{\partial y^2\partial t^2}\right)\end{aligned} \tag{15}$$

Substituting Eq. (3) Into Eq. (7) and the subsequent results into Eq. (11), the equations of motion are obtained in terms of displacements (w_0,θ) as follows compact form

$$\begin{Bmatrix}M\\ N_S\end{Bmatrix}=\begin{Bmatrix}A & B\\ B & A_s\end{Bmatrix}\begin{Bmatrix}k^b\\ k^s\end{Bmatrix},\ N_{Tc}=H\gamma \tag{16}$$

in which

$$M=\left\{M_x\,,M_y,M_{xy}\right\}^t,\ N_s=\left\{N_{sx}\,,N_{sy},N_{sxy}\right\}^t \tag{17a}$$

$$k^b=\left\{k_x^b\,,k_y^b,k_{xy}^b\right\}^t,\ k^s=\left\{k_x^s\,,k_y^s,k_{xy}^s\right\}^t \tag{17b}$$

$$A=\begin{bmatrix}A_{11} & A_{12} & 0\\ A_{12} & A_{22} & 0\\ 0 & 0 & A_{66}\end{bmatrix},\quad B=\begin{bmatrix}B_{11} & B_{12} & 0\\ B_{12} & B_{22} & 0\\ 0 & 0 & B_{66}\end{bmatrix},A_s=\begin{bmatrix}A_{s11} & A_{s12} & 0\\ A_{s12} & A_{s22} & 0\\ 0 & 0 & A_{s66}\end{bmatrix} \tag{18a}$$

$$N_{Tc}=\left\{N_{Tcx}\,,N_{Tcy}\right\}^t,\gamma=\left\{\gamma_{xz}^0\,,\gamma_{yz}^0\right\}^t,\quad H=\begin{bmatrix}H_{44} & 0\\ 0 & H_{55}\end{bmatrix} \tag{18b}$$

and stiffness components are given as

$$\left(A_{ij},B_{ij},A_{sij}\right)=\int_{-h/2}^{h/2}(z^2,zf(z),f(z)^2)C_{ij}dz\,,\quad(i,j=1,2,6) \tag{19a}$$

$$H_{ij}=\int_{-h/2}^{h/2}\acute{f}(z)^2C_{ij}dz\ ,(i,j=4,5) \tag{19b}$$

Introducing Eq. (16) into Eq. (15), the equations of

motion can be expressed in terms of displacements ($w_0$and θ). and the appropriate equations take the form

$$\begin{gathered} A_{11}d_{1111}w_0 - B_{11}K_1\acute{A}d_{1111}\theta + 2A_{12}d_{1122}w_0 - \\ B_{12}\left(K_1\acute{A} + K_2\acute{B}\right)d_{1122}\theta + A_{22}d_{2222}w_0 - \\ B_{22}K_2\acute{B}d_{2222}\theta + 4A_{66}d_{1122}w_0 - 2B_{66}\left(K_1\acute{A} + \right. \\ \left. K_2\acute{B}\right)d_{1122}\theta - q = -I_1\ddot{w}_0 + I_2(d_{11}\ddot{w}_0 + d_{22}\ddot{w}_0) - \\ I_3\left(K_1\acute{A}d_{11}\ddot{\theta} + K_2\acute{B}d_{22}\ddot{\theta}\right) \end{gathered} \tag{20a}$$

$$\begin{gathered} \left(-B_{11}d_{1111}w_0 + A_{s11}K_1\acute{A}d_{1111}\theta - B_{12}d_{1122}w_0 + \right. \\ \left. A_{s12}K_2\acute{B}d_{1122}\theta\right)K_1\acute{A} + \left(-B_{12}d_{1122}w_0 + \right. \\ \left. A_{s12}K_1\acute{A}d_{1122}\theta - B_{22}d_{2222}w_0 + \right. \\ \left. A_{s22}K_2\acute{B}d_{2222}\theta\right)K_2\acute{B} + \left(-2B_{66}d_{1122}w_0 + \right. \\ \left. A_{s66}\left(K_1\acute{A} + \right. K_2\acute{B}\right)d_{1122}\theta\left)\left(K_1\acute{A} + K_2\acute{B}\right) - \right. \\ \left(K_1\acute{A}\right)^2H_{55}d_{11}\theta - \left(K_2\acute{B}\right)^2H_{44}d_{22}\theta = \\ -I_3\left(K_1\acute{A}d_{11}\ddot{w}_0 + \right. K_2\acute{B}d_{22}\ddot{w}_0\left) + I_4\left(\left(K_1\acute{A}\right)^2d_{11}\ddot{\theta} + \right.\right. \\ \left.\left.\left(K_2\acute{B}\right)^2d_{22}\ddot{\theta}\right) \end{gathered} \tag{20b}$$

where d_{ij}, d_{ijl} and d_{ijlm} are the following differential operators

$$\begin{gathered} d_{ij} = \frac{\partial^2}{\partial x_i \partial x_j}\ , d_{ijl} = \frac{\partial^3}{\partial x_i \partial x_j \partial x_l}\ , \\ d_{ijlm} = \frac{\partial^4}{\partial x_i \partial x_j \partial x_l \partial x_m}, d_i = \frac{\partial}{\partial x_i}\ ,(\ i,j,l,m = 1,2) \end{gathered} \tag{21}$$

The shear stresses (τ_{xz}, τ_{yz}) can be expressed by the constitutive relations Eq. (7) or by the integration of the equilibrium equations of 3D elasticity with respect to thickness coordinate

$$\frac{\partial \sigma_x}{\partial x} + \frac{\partial \tau_{xy}}{\partial y} + \frac{\partial \tau_{xz}}{\partial z} = 0 \text{ and } \frac{\partial \tau_{xy}}{\partial x} + \frac{\partial \sigma_y}{\partial y} + \frac{\partial \tau_{yz}}{\partial z} = 0 \tag{22}$$

Integrating Eq. (22) with respect to thickness coordinate z and applying the following boundary conditions at the upper and lower surfaces of the plate

$$[\tau_{xz}]_{z=\pm h/2} = 0 \quad , \quad [\tau_{yz}]_{z=\pm h/2} = 0 \tag{23}$$

In this article it should be noted that:

τ_{xz}^{CR} and τ_{yz}^{CR} are the stresses obtained by the constitutive relations and $(\tau_{xz}^{EE}, \tau_{yz}^{EE})$ are the stresses calculated by the equilibrium equations.

2.4 Analytical solution for simply-supported FG plates

The Navier solution procedure is employed to determine the analytical solutions for which the displacement variables are expressed as product of arbitrary parameters and known trigonometric functions to respect the equations of motion and boundary conditions.

$$\begin{Bmatrix} w_0 \\ \theta \end{Bmatrix} = \sum_{m=1}^{\infty}\sum_{n=1}^{\infty} \begin{Bmatrix} w_{mn}\sin(\lambda x)\sin(\mu y)\sin(\omega_{mn}t) \\ \theta_{mn}\sin(\lambda x)\sin(\mu y)\sin(\omega_{mn}t) \end{Bmatrix} \tag{24}$$

with

$$\lambda = \frac{m\pi}{a} \quad , \quad \mu = \frac{n\pi}{b} \tag{25}$$

Where w_{mn} ; θ_{mn} arbitrary parameters to be determined m, n are mode numbers and ω is frequency of free vibration of the plate, $i = \sqrt{-1}$ the imaginary unit.

The transverse load q is also expanded in the double-Fourier sine series as

-Bending analysis of isotropic plates subjected to uniformly distributed load

$$q(x,y) = \sum_{m=1}^{\infty}\sum_{n=1}^{\infty} q_{mn}sin\left(\frac{m\pi}{a}x\right)sin\left(\frac{n\pi}{b}y\right) \tag{26a}$$

where

$$q_{mn} = \frac{16q_0}{mn\pi^2}\ for\ m = 1,3,5,\dots and\ n = 1,3,5,\dots \tag{26b}$$

$$q_{mn} = 0\ for\ m = 2,4,\dots\dots and\ n = 2,4,\dots\dots \tag{26c}$$

-Bending analysis of isotropic plates subjected to sinusoidal load

$$q(x,y) = q_0\sin\left(\frac{\pi}{a}x\right)\sin\left(\frac{n\pi}{b}y\right) \tag{27}$$

-Bending analysis of isotropic plates subjected to linearly varying load

$$q(x,y) = \sum_{m=1}^{\infty}\sum_{n=1}^{\infty} q_{mn}\sin\left(\frac{m\pi}{a}x\right)\sin\left(\frac{n\pi}{b}y\right) \tag{28a}$$

where

$$\begin{gathered} q_{mn} = -(8q_0/mn\pi^2)\cos(m\pi)\ for\ m \\ = 1,3,5,\dots\dots and\ n = 1,3,5,\dots. \end{gathered} \tag{28b}$$

Substituting Eq. (24) into Eq. (20), the following problem is obtained:

$$\begin{gathered} q(x,y) = q_0\sin\left(\frac{\pi}{a}x\right)\sin\left(\frac{n\pi}{b}y\right) \\ \left(\begin{bmatrix} K_{11} & K_{12} \\ K_{12} & K_{22} \end{bmatrix} - \omega^2\begin{bmatrix} m_{11} & m_{12} \\ m_{12} & m_{22} \end{bmatrix}\right)\begin{Bmatrix} w_{mn} \\ \theta_{mn} \end{Bmatrix} = \begin{Bmatrix} q_{mn} \\ 0 \end{Bmatrix} \end{gathered} \tag{29}$$

where $[K] = \begin{bmatrix} K_{11} & K_{12} \\ K_{12} & K_{22} \end{bmatrix}$ stiffness matrices (23)

and $[M] = \begin{bmatrix} m_{11} & m_{12} \\ m_{12} & m_{22} \end{bmatrix}$ mass matrices.

In which

$$\begin{gathered} K_{12} = -2\left(K_1\acute{A} + K_2\acute{B}\right)B_{66}\lambda^2\mu^2 - \left(K_1\acute{A} + \right. \\ \left. K_2\acute{B}\right)B_{12}\lambda^2\mu^2 - K_1\acute{A}B_{11}\lambda^4 - K_2\acute{B}B_{22}\mu^4 \\ K_{22} = \left(K_1\acute{A}\lambda^4A_{s11} + K_2\acute{B}\lambda^2\mu^2A_{s12}\right)K_1\acute{A} + \\ \left(K_1\acute{A}\right)^2\lambda^2H_{55} + \left(K_1\acute{A}\lambda^2\mu^2A_{s12} + K_2\acute{B}\mu^4A_{s22}\right)K_2\acute{B} + \\ \left(K_2\acute{B}\right)^2\mu^2H_{44} + \left(K_1\acute{A}\lambda^2\mu^2A_{s66} + \right. \\ \left. K_2\acute{B}\lambda^2\mu^2A_{s66}\right)\left(K_1\acute{A} + K_2\acute{B}\right) \\ m_{11} = -I_1 - I_2(\lambda^2 + \mu^2) \\ m_{12} = I_3\left(K_1\acute{A}\lambda^2 + K_2\acute{B}\mu^2\right) \\ m_{22} = -I_4\left(\left(K_1\acute{A}\right)^2\lambda^2 + \left(K_2\acute{B}\right)^2\mu^2\right) \end{gathered} \tag{30}$$

3. Numerical results and discussion

In this section, the results obtained by the present higher order shear deformation theory are compared with those obtained by the other higher order shear deformation

Table 1 Comparison of non-dimensional inplane displacement $(\bar{u})$ at $(x = 0, y = b/2, z = \pm h/2)$, transverse displacement $(\bar{w})$ $(x = a/2, y = b/2, z = 0)$, inplane normal stress $(\bar{\sigma}_x)$ $(x = a/2, y = b/2, z = \pm h/2)$, inplane shear stress $(\bar{\sigma}_{xy})$ $(x = 0, y = 0, z = \pm h/2)$ and transverse shear stress $(\bar{\sigma}_{zx})$ $(x = 0, y = b/2, z = 0)$ in isotropic square plate subjected to uniformly distributed load

S	Theory	Model	$\bar{u}$	$\bar{w}$	$\bar{\sigma}_x$	$\bar{\sigma}_{xy}$	$\bar{\tau}_{zx}^{CR}$	$\bar{\tau}_{zx}^{EE}$
4	**Present**	ESDT	**0.079**	**5.858**	**0.300**	**0.223**	**0.483**	**0.451**
	Sayyad and Ghugal (2012)	ESDT	0.079	5.816	0.300	0.223	0.481	0.472
	Reddy (1984)	HSDT	0.079	5.869	0.299	0.218	0.482	0.452
	Ghugal and Sayyad (2010)	TSDT	0.074	5.680	0.318	0.208	0.483	0.42
	Ghugal and Pawar (2011)	HPSDT	0.079	5.858	0.297	0.185	0.477	0.451
	Mindlin (1951)	FSDT	0.074	5.633	0.287	0.195	0.330	0.495
	Kirchhoff (1850)	CPT	0.074	4.436	0.287	0.195	-	0.495
	Pagano (1970)	Elasticity	0.072	5.694	0.307	-	0.460	-
10	**Present**	ESDT	**0.075**	**4.664**	**0.289**	**0.200**	**0.506**	**0.484**
	Sayyad and Ghugal (2012)	ESDT	0.075	4.658	0.289	0.204	0.494	0.490
	Reddy (1984)	HSDT	0.075	4.666	0.289	0.203	0.492	0.486
	Ghugal and Sayyad (2010)	TSDT	0.073	4.625	0.307	0.195	0.504	0.481
	Ghugal and Pawar (2011)	HPSDT	0.074	4.665	0.289	0.193	0.489	0.486
	Mindlin (1951)	FSDT	0.074	4.670	0.287	0.195	0.330	0.495
	Kirchhoff (1850)	CPT	0.074	4.436	0.287	0.195	-	0.495
	Pagano (1970)	Elasticity	0.073	4.639	0.289	-	0.487	-

Table 2 Comparison of non-dimensional inplane displacement $(\bar{u})$ at$(x = 0, y = b/2, z = \pm h/2)$, transverse displacement $(\bar{w})$ at$(x = a/2, y = b/2, z = 0)$, inplane normal stress$(\bar{\sigma}_x)$at $(x = a/2, y = b/2, z = \pm h/2)$, inplane shear stress $(\bar{\sigma}_{xy})$ at $(x = 0, y = 0, z = \pm h/2)$ and transverse shear stress $(\bar{\sigma}_{zx})$ at $(x = 0, y = b/2, z = 0)$ in isotropic square plate subjected to sinusoidal load

S	Theory	Model	$\bar{u}$	$\bar{w}$	$\bar{\sigma}_x$	$\bar{\sigma}_{xy}$	$\bar{\tau}_{zx}^{CR}$	$\bar{\tau}_{zx}^{EE}$
4	**Present**	ESDT	**0.046**	**3.778**	**0.210**	**0.113**	**0.252**	**0.234**
	Sayyad and Ghugal (2012)	ESDT	0.046	3.748	0.213	0.114	0.238	0.236
	Reddy (1984)	HSDT	0.046	3.787	0.209	0.112	0.237	0.226
	Ghugal and Sayyad (2010)	TSDT	0.044	3.653	0.226	0.133	0.244	0.232
	Ghugal and Pawar (2011)	HPSDT	0.047	3.779	0.209	0.112	0.236	0.235
	Mindlin (1951)	FSDT	0.044	3.626	0.197	0.106	0.159	0.239
	Kirchhoff (1850)	CPT	0.044	2.803	0.197	0.106	-	0.238
	Pagano (1970)	Elasticity	0.049	3.662	0.217	-	0.236	-
10	**Present**	ESDT	**0.044**	**2.959**	**0.200**	**0.108**	**0.254**	**0.238**
	Sayyad and Ghugal (2012)	ESDT	0.044	2.954	0.200	0.108	0.239	0.238
	Reddy (1984)	HSDT	0.044	2.961	0.199	0.107	0.238	0.229
	Ghugal and Sayyad (2010)	TSDT	0.044	2.933	0.212	0.110	0.245	0.235
	Ghugal and Pawar (2011)	HPSDT	0.044	2.959	0.199	0.107	0.237	0.238
	Mindlin (1951)	FSDT	0.044	2.934	0.197	0.106	0.169	0.239
	Kirchhoff (1850)	CPT	0.044	2.802	0.197	0.106	-	0.238
	Pagano (1970)	Elasticity	0.044	2.942	0.200	-	0.238	-

theories of (Reddy 1984, Ghugal and Sayyad 2010, Ghugal and Pawar 2011, Sayyad and Ghugal 2012), and the results determined by first order shear deformation theory (FSDT) of Mindlin (1951), classical plate theory (CPT) of Kirchhoff (1850) and the exact elasticity solution of Pagano (1970).

For convenience, the numerical results for bending and vibration are presented in non-dimensional form by the following relations

$$\bar{u} = \frac{uE_2}{qhS^3}, \bar{w} = \frac{100Ew}{qhS^4}, \ (\bar{\sigma}_x, \bar{\sigma}_y) = \frac{(\sigma_x, \sigma_y)}{qS^2}, \quad \bar{\tau}_{zx} = \frac{\tau_{xz}}{qS}, \ \bar{\omega} = \omega_{mn} h\sqrt{\rho/G} \tag{31}$$

where S (a/h)=Thickness ratio.

The material properties of the isotropic plate are used

$$E = 210 \text{ GPa}, \ \mu = 0.3, \ G = \frac{E}{2(1+\mu)} \text{ and } \rho = 7800 \text{ Kg/m}^3$$

where E is the Young's modulus, G is the shear modulus, μ is the Poisson's ratio and ρ is density of the material.

Example 1: Table1 demonstrates the comparison of inplane displacement, transverse deflection, inplane normal stress, inplane shear stress and transverse shear stress for the isotropic square plate subjected to uniformly distributed load for the various aspect ratios. For aspect ratios (S=a/h) 4 the proposed theory and order theories overestimate the

Table 3 Comparison of non-dimensional inplane displacement $(\bar{u})$ at $(x = 0, y = b/2, z = \pm h/2)$, transverse displacement $(\bar{w})$ at $(x = a/2, y = b/2, z = 0)$, inplane normal stress $(\bar{\sigma}_x)$ at $(x = a/2, y = b/2, z = \pm h/2)$, inplane shear stress $(\bar{\sigma}_{xy})$ at $(x = 0, y = 0, z = \pm h/2)$ and transverse shear stress $(\bar{\sigma}_{zx})$ at $(x = 0, y = b/2, z = 0)$ in isotropic square plate subjected to linearly varying load

S	Theory	Model	$\bar{u}$	$\bar{w}$	$\bar{\sigma}_x$	$\bar{\sigma}_{xy}$	$\bar{\tau}_{zx}^{CR}$	$\bar{\tau}_{zx}^{EE}$
4	**Present**	ESDT	**0.0397**	**2.929**	**0.151**	**0.108**	**0.240**	**0.225**
	Sayyad and Ghugal (2012)	ESDT	0.0396	2.908	0.150	0.111	0.240	0.236
	Reddy (1984)	HSDT	0.0395	2.935	0.150	0.109	0.241	0.226
	Ghugal and Sayyad (2010)	TSDT	0.0370	2.840	0.159	0.104	0.241	0.210
	Ghugal and Pawar (2011)	HPSDT	0.0395	2.929	0.148	0.092	0.239	0.225
	Mindlin (1951)	FSDT	0.0370	2.817	0.144	0.097	0.165	0.247
	Kirchhoff (1850)	CPT	0.0370	2.218	0.144	0.097	-	0.247
	Pagano (1970)	Elasticity	0.0360	2.847	0.153	-	0.230	-
10	**Present**	ESDT	**0.0373**	**2.332**	**0.145**	**0.099**	**0.253**	**0.243**
	Sayyad and Ghugal (2012)	ESDT	0.0375	2.329	0.144	0.102	0.247	0.245
	Reddy (1984)	HSDT	0.0375	2.333	0.144	0.101	0.246	0.243
	Ghugal and Sayyad (2010)	TSDT	0.0365	2.313	0.153	0.097	0.252	0.241
	Ghugal and Pawar (2011)	HPSDT	0.0370	2.332	0.144	0.096	0.245	0.243
	Mindlin (1951)	FSDT	0.0370	2.335	0.143	0.097	0.165	0.248
	Kirchhoff (1850)	CPT	0.0370	2.213	0.143	0.097	-	0.248
	Pagano (1970)	Elasticity	0.0365	2.320	0.144	-	0.244	-

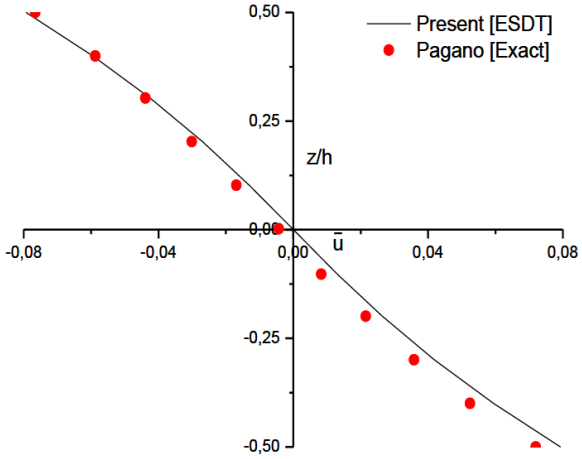

Fig. 2 Through thickness variation of inplane displacement of isotropic plate subjected to uniformly distributed load for aspect ratio 4

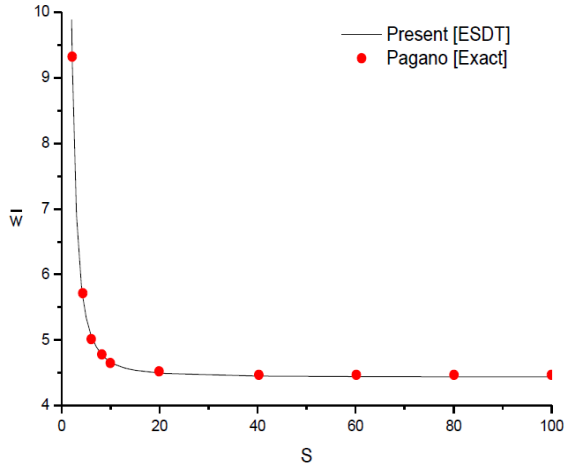

Fig. 3 Through thickness variation of transverse displacement of isotropic plate subjected to uniformly distributed load for aspect ratio 4

results as compared to those of exact solution. For aspect ratio 10, the results obtained are in close agreement with the elasticity solution. Through thickness variations of displacements and stresses are shown in Figs. 2-5. Present theory is in good agreement with the elasticity solution.

Example 2: Table2 shows the displacements and stress for the plate under sinusoidal load. For aspect ratios 4, the current theory and order theories underestimate the results as compared to those of "*exact solution*", The result of inplane displacement predicted by present theory and exact solution is identical for the aspect ratio 10. The thickness variation of "*inplane displacement*" of the plate is presented in Fig. 6.

Example 3: The displacements and stresses of "*simply supported square plate*" under linearly varying load are shown in Table 3 and a very good agreement is demonstrated with exact solution for the aspect ratio 10.

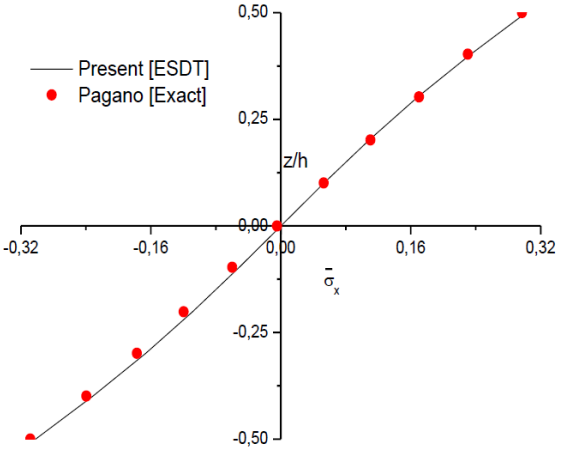

Fig. 4 Through thickness variation of inplane normal stress of isotropic plate subjected to uniformly distributed load for aspect ratio 4

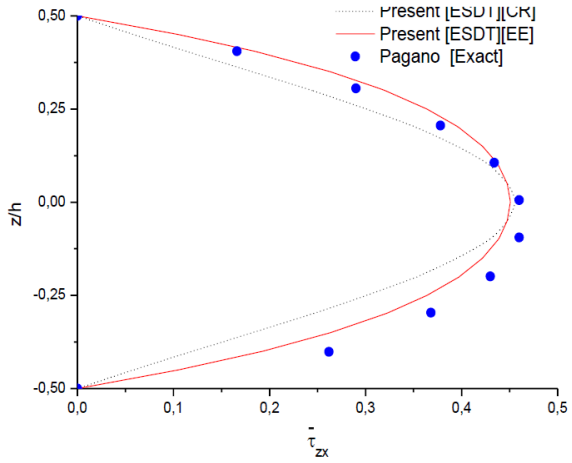

Fig. 5 Through thickness variation of transverse shear stress of isotropic plate subjected to uniformly distributed load for aspect ratio 4

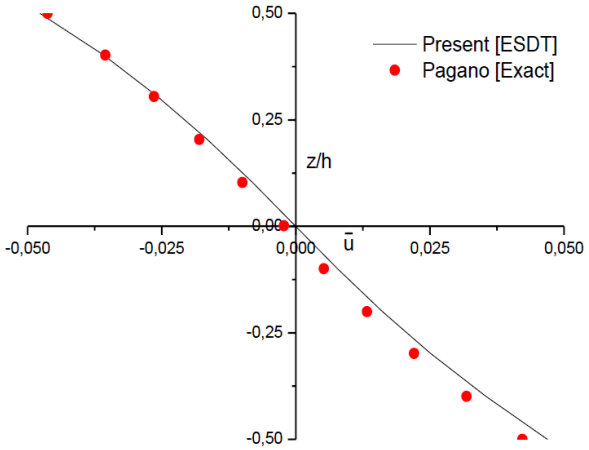

Fig. 6 Through thickness variation of inplane displacement of isotropic plate subjected to single sine load for aspect ratio 4

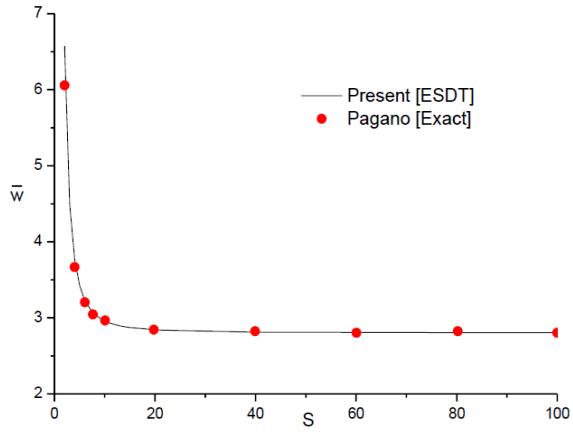

Fig. 7 Through thickness variation of transverse displacement of isotropic plate subjected to single sine load for aspect ratio 4

Through thickness variations of displacements and stress are plotted in Figs. 10-13.

Example 4: The comparison of natural flexural mode frequencies ($\bar{\omega}_w$) and "*thickness shear mode frequencies*" ($\bar{\omega}_\theta$) for simply supported isotropic square plates are presented in Table 4. Present theory is in

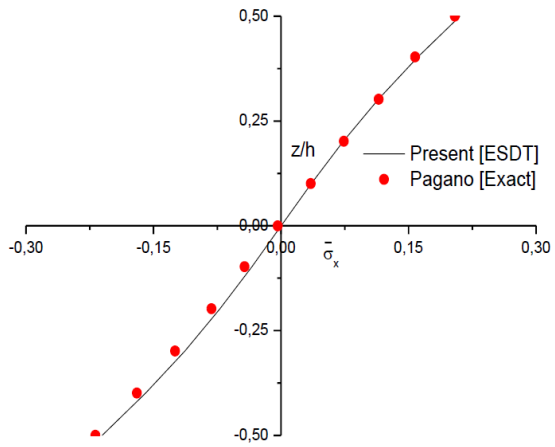

Fig. 8 Through thickness variation of inplane normal stress of isotropic plate subjected to single sine load for aspect ratio 4

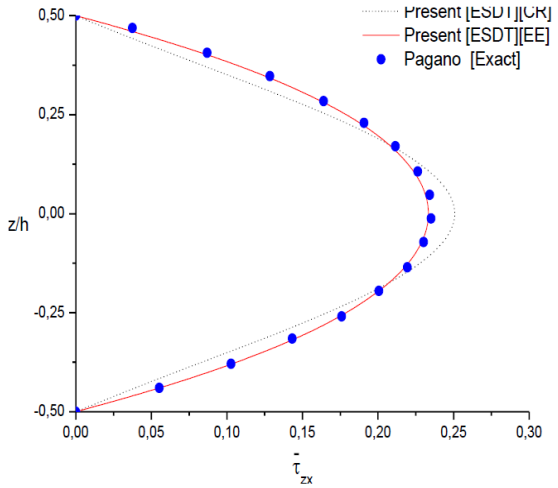

Fig. 9 Through thickness variation of transverse shear stress of isotropic plate subjected to single sine load for aspect ratio 4

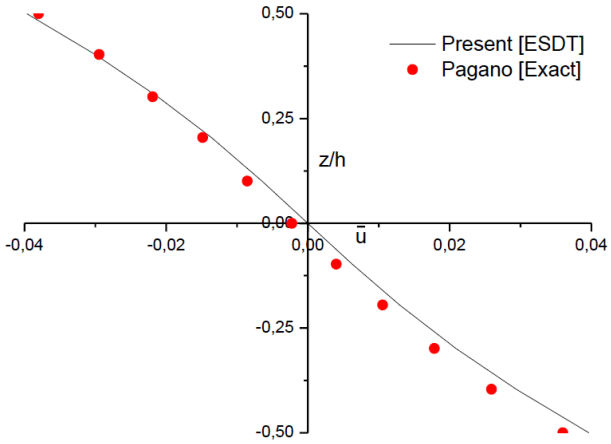

Fig. 10 Through thickness variation of inplane displacement of isotropic plate subjected to linearly varying load for aspect ratio 4

Table 4 Comparison of natural bending mode frequencies $(\bar{\omega}_w)$ and thickness shear mode frequencies $(\bar{\omega}_\theta)$ of simply supported isotropic square plates $(S = 10)$

a/b	$\bar{\omega}$	*(m,n)*	**Present**	Exact (1970)	Sayyad and Ghugal (2012)	Ghugal and Sayyad (2011)	Reddy (1984)	Mindlin (1951)	CPT (1850)
1	$\bar{\omega}_w$	(1,1)	**0.0930**	0.0932	0.0931	0.0933	0.0931	0.0930	0.0955
		(1,2)	**0.2220**	0.2226	0.2223	0.2231	0.2219	0.2219	0.236
		(1,3)	**0.4153**	0.4171	0.4163	0.4184	0.4150	0.4149	0.4629
		(2,2)	**0.3408**	0.3421	0.3415	0.3431	0.3406	0.3406	0.3732
		(2,3)	**0.5213**	0.5239	0.5228	0.5258	0.5208	0.5206	0.5951
		(2,4)	**0.7464**	0.7511	0.7499	0.7542	0.7453	0.7446	0.8926
		(3,3)	**0.6848**	0.6889	0.6874	0.6917	0.6839	0.6834	0.809
		(4,4)	**1.0807**	1.0889	1.0872	1.0945	1.0785	1.0764	1.3716
	$\bar{\omega}_\theta$	(1,1)	**3.2555**	3.2465	3.2428	3.2469	3.2555	3.2538	-
		(1,2)	**3.4123**	3.3933	3.3994	3.394	3.4125	3.4112	-
		(1,3)	**3.6513**	3.6160	3.6381	3.6178	3.6517	3.6510	-
		(2,2)	**3.5586**	3.5298	3.5455	3.5312	3.5589	3.558	-
		(2,3)	**3.7842**	3.7393	3.7709	3.7414	3.7848	3.7842	-
		(2,4)	**4.0712**	4.0037	4.0576	4.0082	4.072	4.072	-
		(3,3)	**3.9921**	3.9310	3.9786	3.9351	3.9928	3.9926	-
		(4,4)	**4.5082**	4.4013	4.4944	4.4102	4.5092	4.5098	-

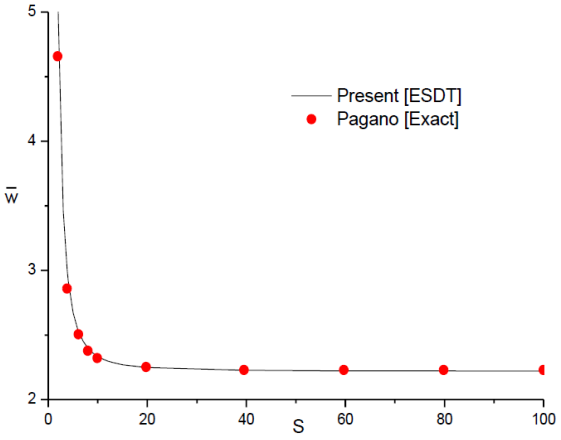

Fig. 11 Through thickness variation of transverse displacement of isotropic plate subjected to linearly varying load for aspect ratio 4

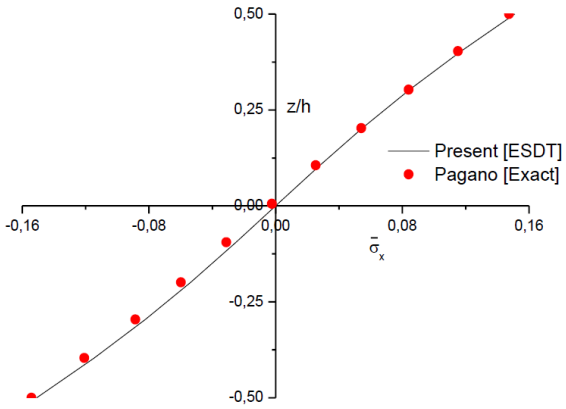

Fig. 12 Through thickness variation of inplane normal stress of isotropic plate subjected to linearly varying load for aspect ratio 4

"*excellent agreement*" of flexural frequencies for different vibrational modes compared to those of "*exact results*",

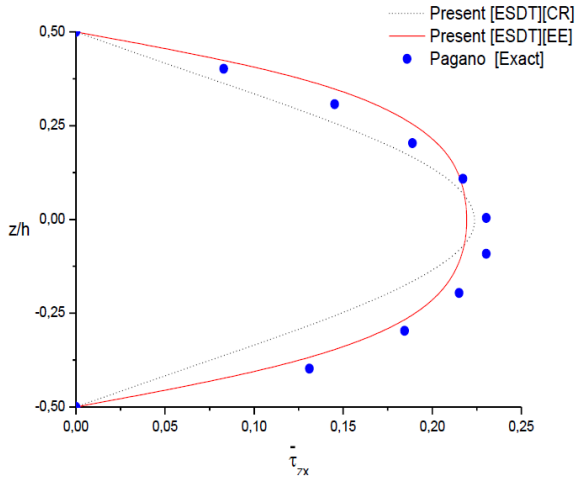

Fig. 13 Through thickness variation of transverse shear stress of isotropic plate subjected to linearly varying load for aspect ratio 4

Comparison of natural flexural mode frequencies $(\bar{\omega}_w)$ of simply supported isotropic rectangular plate is shown in Table 5. Present theory and theory of Reddy (1984) show good accuracy of results, whereas CPT overestimates the flexural frequencies due to neglecting transverse shear deformation influences.

4. Conclusions

The accuracy and efficiency of the present theory has been demonstrated for the flexural and free vibration responses of thick bridge deck. The conclusions of this proposed model are as follows:

- The values of displacements and stresses calculated via the current formulation for different considered loads are in "good agreement" with those of "exact solution",
- The frequencies of flexure and thickness shear modes

Table 5 Comparison of natural bending mode frequencies $(\bar{\omega}_w)$ of simply supported isotropic rectangular plates $(S = 10)$

a/b	$\bar{\omega}$	*(m,n)*	**Present**	Exact (1970)	Sayyad and Ghugal (2012)	Ghugal and Sayyad (2011)	Reddy (1984)	Mindlin (1951)	CPT (1850)
		(1,1)	**0.0703**	0.0704	0.0704	0.0705	0.0704	0.0703	0.0718
		(1,2)	**0.1373**	0.1376	0.1376	0.1393	0.1374	0.1373	0.1427
		(1,3)	**0.2425**	0.2431	0.2433	0.2438	0.2426	0.2424	0.2591
		(1,4)	**0.3785**	0.3800	0.3803	0.3811	0.3789	0.3782	0.4182
		(2,1)	**0.2013**	0.2018	0.2017	0.2023	0.2041	0.2012	0.2128
$\sqrt{2}$	$\bar{\omega}_w$	(2,2)	**0.2627**	0.2634	0.2639	0.2642	0.2628	0.2625	0.2821
		(2,3)	**0.3598**	0.3612	0.3639	0.3623	0.3601	0.3595	0.3958
		(2,4)	**0.4867**	0.4890	0.4928	0.4906	0.4874	0.4861	0.5513
		(3,1)	**0.3971**	0.3987	0.3985	0.3999	0.3975	0.3967	0.4406
		(3,2)	**0.4514**	0.4535	0.4552	0.4550	0.4520	0.4509	0.5073
		(3,3)	**0.5383**	0.5411	0.5465	0.5431	0.5392	0.5375	0.6168

of vibration predicted by the proposed model are in "good agreement" with the exact results for simply supported rectangular plate.

• Compared to the elasticity solution, the novel theory gives more accurate results of bending frequencies for all modes of vibration than the higher order theories.

In conclusion, it can be said that the proposed theory with only two unknowns accurate and simple in solving the bending and vibration responses of thick bridge deck.

References

Ambartsumyan, S.A. (1970), *Theory of Anisotropic Plates*, Technomic Publishing Company, Westport, CT, USA.

Avcar, M. (2019), "Free vibration of imperfect sigmoid and power law functionally graded beams", *Steel Compos. Struct.*, **30**(6), 603-615. http://doi.org/10.12989/scs.2019.30.6.603.

Bert, C.W. and Chen, T.L.C. (1978), "Effect of shear deformation on vibration of antisymmetric angle ply laminated rectangular plates", *Int. J. Solid. Struct.*, **14**(6), 465-473. https://doi.org/10.1016/0020-7683(78)90011-2.

Boulal, A., Bensattalah, T., Karas, A., Zidour, M., Heireche, H. and Adda Bedia, E.A. (2020), "Buckling of carbon nanotube reinforced composite plates supported by Kerr foundation using Hamilton's energy principle", *Struct. Eng. Mech.*, **73**(2), 209-223. https://doi.org/10.12989/sem.2020.73.2.209.

Cuong-Le, T., Nguyen, K.D., Nguyen-Trong, N., Khatir, S., Nguyen-Xuan, H. and Abdel-Wahab, M. (2021), "A three-dimensional solution for free vibration and buckling of annular plate, conical, cylinder and cylindrical shell of FG porous-cellular materials using IGA", *Compos. Struct.*, **259**, 113216. https://doi.org/10.1016/j.compstruct.2020.113216.

Ellali, M., Amara, Kh., Bouazza, M. and Bourada, F. (2018), "The buckling of piezoelectric plates on pasternak elastic foundation using higher-order shear deformation plate theories", *Smart Struct. Syst.*, **21**(1), 113-122. https://doi.org/10.12989/sss.2018.21.1.113.

Ghodrati, B., Yaghootian, A., Ghanbar Zadeh, A. and Sedighi, H.M. (2018), "Lamb wave extraction of dispersion curves in micro/nano-plates using couple stress theories", *Wave. Random Complex Media*, **28**(1), 15-34. https://doi.org/10.1080/17455030.2017.1308582.

Ghugal, Y.M. and Pawar, M.D. (2011), "Buckling and vibration of plates by hyperbolic shear deformation theory", *J. Aerosp. Eng. Technol.*, **1**, 1-12.

Ghugal, Y.M. and Sayyad, A.S. (2010), "Free vibration of thick orthotropic plates using trigonometric shear deformation theory", *Lat. Am. J. Solid. Struct.*, **8**, 229-243.

Hadji, L., Hassaine Daouadji, T., Ait Amar Meziane, M., Tlidji, Y. and AddaBedia, E.A. (2016), "Analysis of functionally graded beam using a new first-order shear deformation theory", *Struct. Eng. Mech.*, **57**(2), 315-325. https://doi.org/10.12989/sem.2016.57.2.315.

Kant, T. and Swaminathan, K. (2001), "Analytical solutions for free vibration of laminated composite and sandwich plates based on a higher-order refined theory", *Compos. Struct.*, **53**(1), 73-85. https://doi.org/10.1016/S0263-8223(00)00180-X.

Khatir, S., Tiachacht, S., Thanh, C.L., Bui, T.Q. and Wahab, M.A. (2019), "Damage assessment in composite laminates using ANN-PSO-IGA and Cornwell indicator", *Compos. Struct.*, **230**, 111509. https://doi.org/10.1016/j.compstruct.2019.111509.

Khatir, S., Tiachacht, S., Thanh, C.L., Ghandourah, E. and Wahab, M.A. (2021), "An improved artificial neural network using arithmetic optimization algorithm for damage assessment in FGM composite plates", *Compos. Struct.*, **273**, 114287. https://doi.org/10.1016/j.compstruct.2021.114287.

Kirchhoff, G. (1850), "Über das Gleichgewicht und die Bewegung einer elastischen Scheibe", *Journal für die reine und angewandte Mathematik (Crelles Journal)*, **1850**(40), 51-88.

Kirchhoff, G.R. (1850), "Uber die Schwingungen einer kriesformigen elastischen Scheibe", *Annalen der Physik und Chemie*, **81**, 258-264.

Madenci, E. (2019), "A refined functional and mixed formulation to static analyses of FGM beams", *Struct. Eng. Mech.*, **69**(4), 427-437. http://doi.org/10.12989/sem.2019.69.4.427.

Mantari, J.L. and Granados, E.V. (2015), "A refined FSDT for the static analysis of functionally graded sandwich plates", *Thin Wall. Struct.*, **90**, 150-158. https://doi.org/10.1016/j.tws.2015.01.015.

Mindlin, R.D. (1951), "Influence of rotary inertia and shear on flexural motions of isotropic, elastic plates", *J. Appl. Mech.*, **18**, 31-38. https://doi.org/10.1115/1.4010217.

Mohan, P.R., Naganarayana, B.P. and Prathap, G. (1994), "Consistent and variationally correct finite elements for higher-order laminated plate theory", *Compos. Struct.*, **29**(4), 445-456. https://doi.org/10.1016/0263-8223(94)90113-9.

Pagano, N.J. (1970), "Exact solutions for bidirectional composites and sandwich plates", *J. Compos. Mater.*, **4**, 20-34. https://doi.org/10.1177/002199837000400102.

Pinto, V.T., Oliveira Rocha, L.A., Fragassa, C., Domingues dos Santos, E. and Isoldi, L.A. (2020), "Multiobjective geometric analysis of stiffened plates under bending through constructal design method", *J. Appl. Comput. Mech.*, **6**(SI), 1438-1449.

https://doi.org/10.22055/jacm.2020.35248.2608.
Reddy, J.N. (1979), "Free vibration of antisymmetric angle ply laminated plates including transverse shear deformation by the finite element method", *J. Sound Vib*., **66**(4), 565-576. https://doi.org/10.1016/0022-460X(79)90700-4.
Reddy, J.N. (1984), "A simple higher order theory for laminated composite plates", *ASME J. Appl. Mech.*, **51**, 745-752. https://doi.org/10.1115/1.3167719.
Reddy, J.N. and Khdeir, A.A. (1989), "Buckling and vibration of laminated composite plates using various plate theories", *AIAA J.*, **27**(12), 1808-1817. https://doi.org/10.2514/3.10338.
Reissner, E. (1945), "The effect of transverse shear deformation on the bending of elastic plates", *ASME J. Appl. Mech.*, **12**, 69-77. https://doi.org/10.1115/1.4009435.
Saadatmorad, M., Jafari-Talookolaei, R.A., Pashaei, M.H. and Khatir, S. (2021), "Damage detection on rectangular laminated composite plates using wavelet based convolutional neural network technique", *Compos. Struct*., **278**, 114656. https://doi.org/10.1016/j.compstruct.2020.113216.
Sallai, B., Hadji, L., Hassaine Daouadji, T. and Adda Bedia, E.A. (2015), "Analytical solution for bending analysis of functionally graded beam", *Steel Compos. Struct*., **19**(4), 829-841. https://doi.org/10.12989/scs.2015.19.4.829.
Sayyad, A.S. and Ghugal, Y.M. (2012), "Bending and free vibration analysis of thick isotropic plates by using exponential shear deformation theory", *Appl. Comput. Mech.*, **6**, 65-82.
Shahrjerdi, A., Mustapha, F., Bayat, M. and Majid, D.L.A. (2011), "Free vibration analysis of solar functionally graded plates with temperature-dependent material properties using second order shear deformation theory", *J. Mech. Sci. Technol*., **25**(9), 2195-2209. https://doi.org/10.1007/s12206-011-0610-x.
Shankara, C.A. and Iyengar, N.G. (1996), "A C^0 element for the free vibration analysis of laminated composite plates", *J. Sound Vib.*, **191**(5), 721-738. https://doi.org/10.1006/jsvi.1996.0152.
Srinivas, S., JogaRao, C.V. and Rao, A.K. (1970), "An exact analysis for vibration of simpply supported homogeneous and laminated thick rectangular plates", *J. Sound Vib.*, **12**, 187-199. https://doi.org/10.1016/0022-460X(70)90089-1.
Sun, C.T. and Whitney, J.M. (1973), "Theories for the dynamic response of laminated plates", *AIAA J*., **11**(2), 178-183. https://doi.org/10.2514/3.50448.
Swaminathan, K. and Naveenkumar, D.T. (2014), "Higher order refined computational models for the stability analysis of FGM plates: Analytical solutions", *Eur. J. Mech. A/Solid.*, **47**, 349-361. https://doi.org/10.1016/j.euromechsol.2014.06.003.
Ton, T.H.L. (2020), "A novel quadrilateral element for dynamic response of plate structures subjected to blast loading", *J. Appl. Comput. Mech.*, **6**, 1314-1323.
Touratier, M. (1991), "An efficient standard plate theory", *Int. J. Eng. Sci.*, **29**(8), 901-916. https://doi.org/10.1016/0020-7225(91)90165-Y.
Tran-Ngoc, H., Khatir, S., Ho-Khac, H., De Roeck, G., Bui-Tien, T. and Wahab, M.A. (2020), "Efficient Artificial neural networks based on a hybrid metaheuristic optimization algorithm for damage detection in laminated composite structures", *Compos. Struct*., **262**, 113339. https://doi.org/10.1016/j.compstruct.2020.113339.
Vinyas, M. (2020), "On frequency response of porous functionally graded magneto-electro-elastic circular and annular plates with different electro-magnetic conditions using HSDT", *Compos. Struct.*, **240**, 112044. https://doi.org/10.1016/j.compstruct.2020.112044.
Viswanathan, K.K., Javed, S. and Abdul Aziz, Z. (2013), "Free vibration of symmetric angle-ply layered conical shell frusta of variable thickness under shear deformation theory", *Struct. Eng. Mech*., **45**(2), 259-275. http://doi.org/10.12989/sem.2013.45.2.259.
Whitney, J.M. (1969), "The effect of transverse shear deformation on the bending of laminated plates", *J. Compos. Mater*., **3**(3), 534-547. https://doi.org/10.1177/002199836900300316.
Whitney, J.M. and Pagano, N.J. (1970), "Shear deformation in heterogeneous anisotropic plates", *J. Appl. Mech.-T*, ASME, **37**(4), 1031-1036. https://doi.org/10.1115/1.3408654.
Yaghoobi, H., Valipour, M.S., Fereidoon, A. and Khoshnevisrad, P. (2014), "Analytical study on postbuckling and nonlinear free vibration analysis of FG beams resting on nonlinear elastic foundation under thermo-mechanical loadings using VIM", *Steel Compos. Struct*., **17**(5), 753-776. http://doi.org/10.12989/scs.2014.17.5.753.
Yan, P.C., Norris, C.H. and Stavsky, Y. (1966), "Elastic wave propagation in heterogeneous plates", *Int. J. Solid. Struct*., **2**(4), 665-684. https://doi.org/10.1016/0020-7683(66)90045-X.
Zenzen, R., Khatir, S., Belaidi, I., Le Thanh, C. and Abdel Wahab, M. (2020), "A modifed transmissibility indicator and Artifcial Neural Network for damage identifcation and quantifcation in laminated composite structures", *Comput. Struct*., **248**, 112497. https://doi.org/10.1016/j.compstruct.2020.112497.
Zouatnia, N. and Hadji, L. (2019), "Static and free vibration behavior of functionally graded sandwich plates using a simple higher order shear deformation theory", *Adv. Mater. Res.*, **8**(4), 313-335. https://doi.org/10.12989/amr.2019.8.4.313.

CC

sciendo

Mathematical Modelling in Civil Engineering
Vol. 16-No. 1 : 13-21-2021
Doi: 10.2478/mmce-2021-0007

INVESTIGATION OF RC BEAMS REHABILITATED WITH ANGLE-PLY COMPOSITE LAMINATE PLATE

Kamel ANTAR- PhD Student, Department of Civil Engineering, University of Sidi Bel Abbes, Algeria, e-mail: antarkamel@gmail.com

Khaled AMARA- Lecturer, Professor, Department of Civil Engineering, University of Ain Temouchent, Engineering and Sustainable Development Laboratory, Algeria, e-mail: amara3176@yahoo.fr

Fatima Zohra DJIDAR- PhD Student, Department of Civil Engineering, University of Ain Temouchent, Smart Structures Laboratory, Algeria, e-mail: djidarfatimazohra@gmail.com

Abstract: This parametric study investigates the RC Beams Rehabilitated with angle-ply composite laminate plate $[\theta n/90m]_s$. This work is based on a simple theoretical model to estimate the interfacial stresses developed between the concrete beam and the composite with taking into account the hygrothermal effect. Fibre orientation angle, effects of number of 90° layers and effects of plate thickness and length on the distributions of interfacial stress in the concrete beams reinforced with composite plates have also been studied.

Keywords: Interfacial stresses, Concrete beam, Angle-ply laminates, hygrothermal effects, Fibre volume fractions

1. Introduction

The use of the composite fiber-reinforced plastic (FRP) become more and more very effective given its simplicity. Many studies have been conducted, to predict the interfacial stresses, see, for example, those by Tounsi et al. [1], Tounsi [2], Benyoucef et al. [3], Vilnay [4], Roberts [5], Roberts et al. [6], Malek et al. [7], Robinovitch et al. [8], Ye [9], Smith et al. [10], Barnes et al. [11], Stratford et al. [12]. Bouazaoui [13] have studied the interfacial shear strength between the steel bar surface and concrete surface of steel rods bonded into concrete. Many approximate closed-form solutions have been developed in the past decade for the interfacial stresses in beams bonded with FRP plate [14-17].

The solution presented by Smith et al [18] seems to be the more accurate widely applicable solution, particularly when the flexural stiffness of the bonded plate becomes significant. Rabinovich et al. [8] have presented a higher order analysis in which the adhesive layer was treated as an elastic medium with negligible longitudinal stiffness.

This leads to uniform stresses and linearly varying normal stresses through the thickness of the adhesive layer. The significance of their solution is that it is the first solution that satisfies the stress-free boundary condition at the ends of the adhesive layer. Using the same approach, they investigated the effects of an uneven adhesive layer and material nonlinearity [19]. Shen et al. [20] proposed an alternative analytical complementary energy approach, which resulted in closed-form expressions.

Recently, many authors have conducted a numerical study in different directions to illustrate the principal parameters in order to estimate the distributions of interfacial stress in beams reinforced with composite plates [21-27].

The analytical models present often the assumption of constant environment conditions, while the RC beam and the FRP are subjected to changing temperature and moisture conditions and it should be including in the analysis [28]. In this paper, the hygrothermal effects in the concrete beam and the soffit plate will be included to estimate the interfacial shear and normal stresses.

For this case, we introduce an analytical solution which include the mechanical properties of the beam, the plate and the adhesive layer under thermal (temperature effect) and hygroscopic (moisture effect) conditions. The most used solution is Teng's solution Smith et al. [18].

This solution doesn't consider the fibre volume fractions and orientation contrary to Tounsi solution [2] which will be used in this paper. The total interfacial stress is the sum of Tounsi solution and the additional one due to the hygrothermal deformation of the beam and the plate.

2. Governing equations

Fig. 1 shows, a concrete beam (Adherend 1) strengthened by FRP plate (Adherend 2) and bounded by an adhesive layer. This beam is simply supported reinforced beam and subjected to a uniform distributed load.

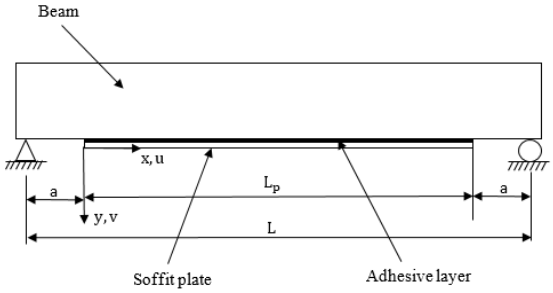

Fig.1. Soffit-plated beam

The following assumptions are used:

- The materials concrete beam, FRP plate and adhesive are linear elastic.
- Shear and normal stresses in the adhesive layer are constant across its thickness.
- The curvature in the beam and the plate are same.

The Fig. 2 represents a differential segment of plated beam. τ(x) and σ(x) are the interfacial shear and normal stresses respectively with positive sign convention for the bending moment, shear force, axial force and applied loading. The derivation of the new solution below is described in terms of adherends 1 and 2, where adherend 1 is the beam and adherend 2 is the soffit plate.

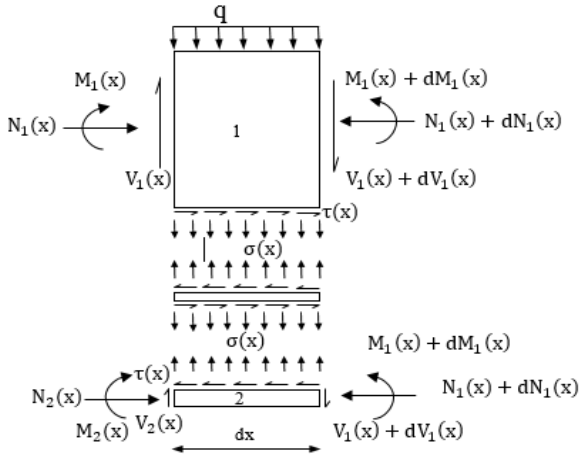

Fig.2. Differential segment of a soffit-plated beam

The shear strain ϒ in the adhesive layer can be written as

$$\Upsilon = \frac{du(x,y)}{dy} + \frac{dv(x,y)}{dx} \tag{1}$$

u(x,y) and v(x,y) are the horizontal and vertical displacements of the adhesive layer respectively. τ(x) is given as

$$\tau(x) = G_a\left(\frac{du(x,y)}{dy} + \frac{dv(x,y)}{dx}\right) \quad (2)$$

where G_a is the shear modulus of the adhesive layer. Differentiating the expression (2) with respect to x gives

$$\frac{d\tau(x)}{dx} = G_a\left(\frac{d^2u(x,y)}{dy} + \frac{d^2v(x,y)}{dx}\right) \quad (3)$$

The curvature is function of the applied moment $M_T(x)$

$$\frac{d^2v(x)}{dx^2} = -\frac{1}{(EI)_t}M_T(x) \quad (4)$$

where $(EI)_t$ is the total flexural rigidity of the composite section. u(x,y) must vary linearly across the adhesive thickness t_a , then

$$\frac{du}{dy} = \frac{1}{t_a}[u_2(x) - u_1(x)] \quad (5)$$

where $u_1(x)$ and $u_2(x)$ are the longitudinal displacements at the base of adherend 1 and the top of adherend 2, respectively. Eq. (3) can be rewritten as

$$\frac{d\tau(x)}{dx} = G_a\left(\frac{du_2(x)}{dx} - \frac{du_1(x)}{dx} - \frac{t_a}{(EI)_t}M_T(x)\right) \quad (6)$$

The third term in parentheses in Eq. (6) can be ignored Smith et al. [10] in the following derivation. The strains at the base of adherend 1 and the top of adherend 2 taking account the hygrothermal deformations are given as

$$\varepsilon_1(x) = \frac{du_1(x)}{dx} = \frac{y_1}{E_1I_1}M_1(x) - \frac{1}{E_1A_1}N_1(x) + \alpha_1\Delta T + \beta_1\Delta C \quad (7)$$

Where α_1 is the coefficient of thermal expansion and β_1 is the coefficient of hygroscopic expansion of the RC beam. ΔT and ΔC are the temperature and percent moisture change respectively.

The laminate theory is used to estimate the strain of the symmetrical composite plate [28], i.e.

$$\varepsilon_x^0 = A_{11}^{'}N_x\frac{1}{b_2} \quad ; \quad k_x = D_{11}^{'}M_x\frac{1}{b_2} \quad (8)$$

[A'] is the inverse of the extensional matrix [A]; [D'] is the inverse of the flexural matrix; b_2 is a width of FRP plate. Using CLT, the strain at the top of the FRP plate 2 is given as

$$\varepsilon_2(x) = \varepsilon_x^0 - k_x\frac{t_2}{2} + \alpha_2\Delta T + \beta_2\Delta C \quad (9)$$

Substituting Eq. (9) in (10) gives the following equation:

$$\varepsilon_2(x) = -D_{11}^{'}\frac{t_2}{2b_2}M_2(x) + \frac{A_{11}^{'}}{b_2}N_2(x) + \alpha_2\Delta T + \beta_2\Delta C \quad (10)$$

Considering horizontal equilibrium gives

$$\frac{dN_1(x)}{dx} = \frac{dN_2(x)}{dx} = b_2\tau(x) \quad (11)$$

where

$$N_1(x) = N_2(x) = N(x) = b_2\int_0^x \tau(x)dx \quad (12)$$

And the moment equilibrium of the differential segment of the plated beam in Fig. 2 gives

$$M_T(x) = M_1(x) + M_2(x) + N(x)(y_1 + y_2 + t_a) \quad (13)$$

The bending moment in each adherend is function of the total applied moment and the interfacial shear stress as

$$M_1(x) = \frac{R}{R+1}\left[M_T(x) - b_2\int_0^x \tau(x)(y_1 + y_2 + t_a)dx\right] \quad (14)$$

$$M_2(x) = \frac{1}{R+1}\left[M_T(x) - b_2\int_0^x \tau(x)(y_1 + y_2 + t_a)dx\right] \quad (15)$$

The first derivative of the bending moment in each adherend gives

$$\frac{dM_1(x)}{dx} = V_1(x) = \frac{R}{R+1}[V_T(x) - b_2\tau(x)(y_1 + y_2 + t_a)] \quad (16)$$

$$\frac{dM_2(x)}{dx} = V_2(x) = \frac{1}{R+1}[V_T(x) - b_2\tau(x)(y_1 + y_2 + t_a)] \quad (17)$$

Substituting Eqs. (7) and (9) into Eq. (6) and differentiating the resulting equation once yields

$$\frac{d^2\tau(x)}{dx^2} = \frac{G_a}{t_a}\left(\frac{-t_2}{2b_2}D'_{11}\frac{dM_2(x)}{dx} + \frac{A'_{11}}{b_2}\frac{dN_2(x)}{dx} - \frac{y_1}{E_1I_1}\frac{dM_1(x)}{dx} + \frac{1}{E_1A_1}\frac{dN_1(x)}{dx}\right) \quad (18)$$

Substitution of the shear forces [Eqs. (16) and (17)] and axial forces [Eq. (12)] in both adherends into Eq. (18) gives the following governing differential equation for the interfacial shear stress:

$$\frac{d^2\tau(x)}{dx^2} - \frac{G_a}{t_a}\left(A'_{11} + \frac{b_2}{E_1I_1} + \frac{(y_1 + y_2)(y_1 + y_2 + t_a)}{E_1I_1D'_{11} + b_2}b_2D'_{11}\tau(x)\right) + \frac{G_a}{t_a}\left(\frac{(y_1 + y_2)}{E_1I_1D'_{11} + b_2}D'_{11}\right)V_T(x) = 0 \quad (19)$$

For simplicity and for such loading, $\frac{d^2V_T(x)}{dx^2} = 0$, the general solution of Eq. (19) is given by

$$\tau(x) = B_1\cosh(\lambda x) + B_2\sin h(\lambda x) + m_1V_T(x) \quad (20)$$

where

$$\lambda^2 = \frac{G_a}{t_a}\left(A'_{11} + \frac{b_2}{E_1A_1} + \frac{(y_1+y_2)(y_1+y_2+t_a)}{E_1I_1D'_{11}+b_2}b_2D'_{11}\right) \quad (21)$$

and

$$m_1 = \frac{G_a}{t_a\lambda^2}\left(\frac{y_1 + y_2}{E_1I_1D'_{11} + b_2}D'_{11}\right) \quad (22)$$

The general solution for the interfacial shear stress for a simply supported beam subjected to a uniformly distributed load is given as

$$\tau(x) = B_1\cosh(\lambda x) + B_2\sin h(\lambda x) + m_1V_T(x) \quad (23)$$

The constants of integration need to be determined by applying suitable boundary conditions. At x=0. Here, the moment at the plate end $M_2(0) = N_1(0) = N_2(0) = 0$ and as a result

$$M_1(0) = M_T(0) = \frac{qa}{2}(L - a) \quad (24)$$

Substituting Eqs. (7) and (10) into Eq. (6) with the third term ignored, and applying the above boundary condition, gives

$$\left.\frac{d\tau(x)}{dx}\right|_{x=0} = -m_2M_T(0) \quad (25)$$

where

$$m_2 = \frac{G_ay_1}{t_aE_1I_1} \quad (26)$$

By substituting Eq. (23) into Eq. (28), B_2 can be determined as

$$B_2 = -\frac{m_2qa}{2\lambda}(L - a) + \frac{m_1}{\lambda}q + \frac{G_a}{t_a\lambda}[(\alpha_1 - \alpha_2)\Delta T + (\beta_1 - \beta_2)\Delta C] = -B_1 \quad (27)$$

The normal stress in the adhesive layer, σ(x), is given as

$$\sigma(x) = \frac{E_a}{t_a}[v_2(x) - v_1(x)] \quad (28)$$

where $v_1(x)$ and $v_2(x)$ are the vertical displacements of adherend 1 and 2, respectively.

Differentiating Eq. (28) twice results in

$$\frac{d^2\sigma(x)}{dx^2} = K_n\left[\frac{d^2v_1(x)}{dx^2} - \frac{d^2v_2(x)}{dx^2}\right] \quad (29)$$

Considering the moment–curvature relationships for the beam to be strengthened and the external reinforcement, respectively:

$$\frac{d^2 v_1(x)}{dx^2} = -\frac{1}{E_1 I_1} M_1(x) \quad ; \quad \frac{d^2 v_2(x)}{dx^2} = -\frac{D'_{11}}{b_2} M_2(x) \tag{30}$$

The equilibrium of adherend 1 and 2, leads to the following relationships:

Adherend 1:

$$\frac{dM_1(x)}{dx} = V_1(x) - b_2 y_1 \tau(x) ; \quad \frac{dV_1(x)}{dx} = -b_2 \sigma(x) - q \tag{31}$$

Adherend 2:

$$\frac{dM_2(x)}{dx} = V_2(x) - b_2 \frac{t_2}{2} \tau(x) ; \quad \frac{dV_2(x)}{dx} = b_2 \sigma(x) \tag{32}$$

Based on the above equilibrium equations, the governing differential equations for the deflection of adherends 1 and 2, expressed in terms of the interfacial shear and normal stresses, are given as follows:

Adherend 1:

$$\frac{d^4 v_1(x)}{dx^4} = -\frac{1}{E_1 I_1} b_2 \sigma(x) + \frac{y_1}{E_1 I_1} b_2 \frac{d\tau(x)}{dx} + \frac{q}{E_1 I_1} \tag{33}$$

Adherend 2:

$$\frac{d^4 v_2(x)}{dx^4} = -D'_{11} \sigma(x) + D'_{11} y_2 \frac{d\tau(x)}{dx} + \frac{q}{E_1 I_1} \tag{34}$$

Substitution of Eqs. (33) and (34) into the fourth derivation of the interfacial normal stress obtainable from

Eq. (28) gives the following governing differential equation for the interfacial normal stress:

$$\frac{d^4 \sigma(x)}{dx^4} + \frac{E_a}{t_a}\left(D'_{11} + \frac{b_2}{E_1 I_1}\right)\sigma(x) - \frac{E_a}{t_a}\left(D'_{11} y_2 - \frac{y_1 b_2}{E_1 I_1}\right)\frac{d\tau(x)}{dx} + \frac{q E_a}{t_a E_1 I_1} = 0 \tag{35}$$

The general solution to this fourth-order differential equation is

$$\sigma(x) = e^{-\beta x}\left[C_1 \cos(\beta x) + C_2 \sin(\beta x)\right] - n_1 \frac{d\tau(x)}{dx} - n_2 q \tag{36}$$

where

$$\beta = \sqrt[4]{\frac{E_a}{4 t_a}\left(\frac{b_2}{E_1 I_1} + D'_{11}\right)} \tag{37}$$

and

$$n_1 = \frac{y_1 b_2 - D'_{11} E_1 I_1 y_1}{D'_{11} E_1 I_1 + b_2} \tag{38}$$

$$n_2 = \frac{1}{D'_{11} E_1 I_1 + b_2} \tag{39}$$

As is described by Smith et al. [18], the constants C_1 and C_2 in Eq. (36) are determined using the appropriate boundary conditions:

$$C_1 = \frac{E_a}{2\beta^3 t_{a_1}} \frac{1}{E_1 I_1}\left[V_T(0) + \beta M_T(0)\right] - \frac{n_3}{2\beta^3}\tau(0) + \frac{n_1}{2\beta^3}\left(\left.\frac{d^4\tau(x)}{dx^4}\right|_{x=0} + \beta \left.\frac{d^3\tau(x)}{dx^3}\right|_{x=0}\right) \tag{40}$$

$$C_2 = \frac{E_a}{2\beta^2 t_a} \frac{1}{E_1 I_1} M_T(0) - \frac{n_1}{2\beta^2} \left.\frac{d^3\tau(x)}{dx^3}\right|_{x=0} \tag{41}$$

where

$$n_3 = \frac{E_a b_2}{t_a}\left(\frac{y_1}{E_1 I_1} - \frac{D'_{11} t_2}{2 b_2}\right) \tag{42}$$

3. Results and discussion of the parametric study

Numerical results, obtained by programming with Maple, are presented to illustrate and examine both thermal and hygroscopic effects on the interfacial shear and normal stresses. We consider an RC beam of 3000 mm of length, a soffit plate of LP=2400mm, a uniform distributed load q=50KN/ml. The other geometric parameters and mechanicals properties are resumed in Table1.

Table 1

Geometric and mechanicals properties

Component	Width (mm)	Depth (mm)	Young's Modulus (GPa)	Poisson's ratio
RC beam	200	300	30	
Soffit plate	200	4	50	
Adhesive layer	200	4	2	0.35

3.1. Fibre orientation

The fibre orientation affect significantly the development if interfacial stresses. It's shown in Fig. 3 and Fig. 4 that the shear and normal stresses decrease when the temperature ΔT and percent moisture ΔC decrease and the angle of orientation θ increases.

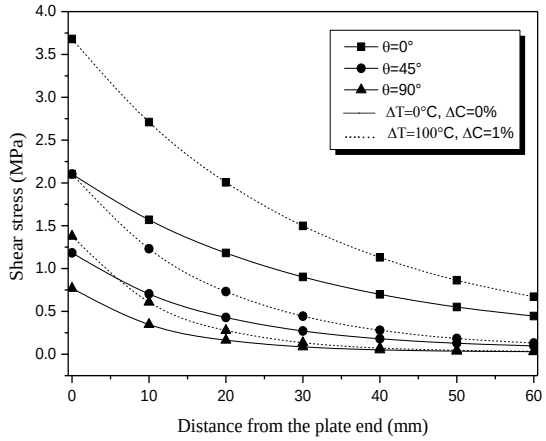

Fig.3. Effect of fibre orientations on shear stress for different hygroscopic cases

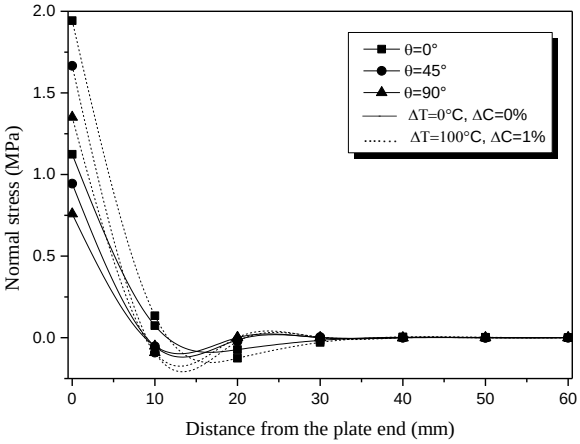

Fig.4. Effect of fibre orientations on normal stress for different hygroscopic cases

3.2. Effect of fibre volume fractions

It is well known in many studies [29-31] that the material properties are function of temperature and moisture. In terms of a micro-mechanical model of laminate, the material properties may be written as [32]

$$E_L = V_f E_f + V_m E_m$$

$$\frac{1}{E_T} = \frac{V_f}{E_f} + \frac{V_m}{G_m} - V_f V_m \frac{\left(\nu_f^2 E_m / E_f\right) + \left(\nu_m^2 E_f / E_m\right) - 2\nu_f \nu_m}{V_f E_f + V_m E_m}$$

$$\frac{1}{G_{LT}} = \frac{V_f}{G_f} + \frac{V_m}{G_m}$$

In the above equations, Vf and Vm are the fibre and matrix volume fractions and are related by :

$$V_f + V_m = 1$$

E_f , G_f and ν_f are the Young's modulus, shear modulus and poisson's ration, respectively, of the fibre, and

E_m , G_m and ν_m are corresponding properties for the matrix.

It is assumed that E_m is a function of temperature and moisture, then E_L, E_T and G_{LT} are also functions of temperature and moisture.

The thickness of each ply is 0.125mm and the material properties adopted are [32] : E_f*=230 GPa,* G_f*=9.0 GPa,* ν_f *=0.203,* ν_m *=0.34* et E_m*= (3.51-0.003T-0.142C)GPa.*In which $T=T_0+\Delta T$ and T_0*=25°C* (room temperature), and $C=C_0+\Delta C$ and C_0*=0 wt% H_2O.*

In addition, three values of fibre volume fractions V_f= (0.5 ; 0.6 et 0.7) are considered.

Fig. 5 and Fig. 6 show the effect of fiber volume fractions V_f on the development of interface constraints.

It can be noted that the shear stress increases by increasing the fiber volume fractions, while no significant change was observed in the normal stresses for the two hygrothermal cases.

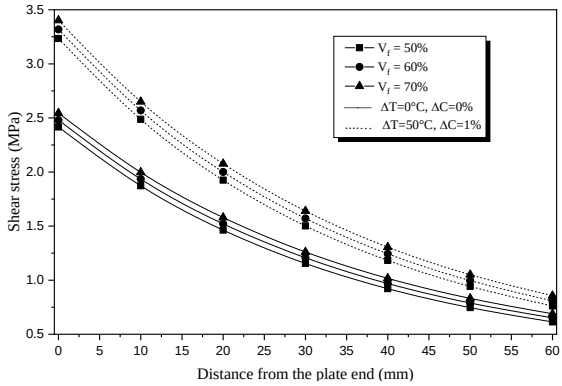

Fig.5. Effect of fibre volume fractions on the shear stresses for a reinforced concrete beam with bonded plate in laminated composite $[0/90]_s$ for different hygrothermal cases.

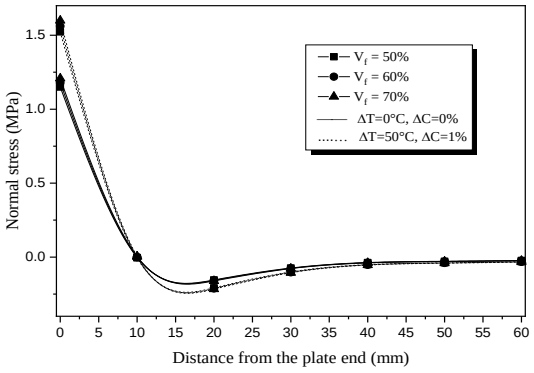

Fig.6. Effect of fibre volume fractions on the normal stress for a reinforced concrete beam with bonded plate in laminated composite $[0/90]_s$ for different hygrothermal cases.

3.3. Plate thickness

Fig. 7 and Fig. 8 show the effects of the plate thickness t_2 on the interfacial stresses. It seen that this plate considerably the normal stress and hardly the shear stress concentration. The normal stress increase with increasing the plate thickness.

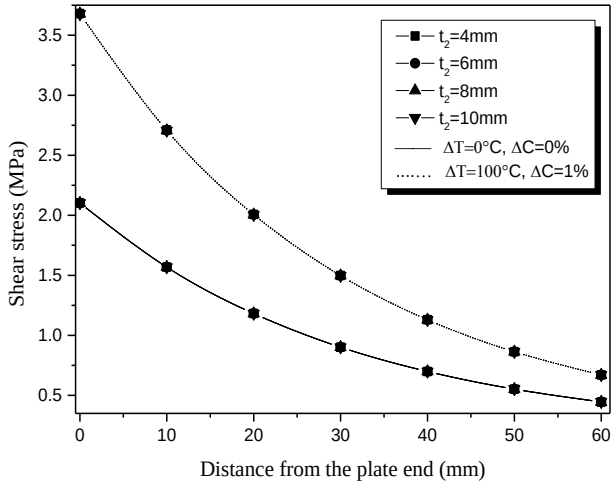

Fig.7 Effect of plate thickness on shear stress for an RC beam with a bonded composites laminates plate $[0/90]_s$ under hygrothermal effect.

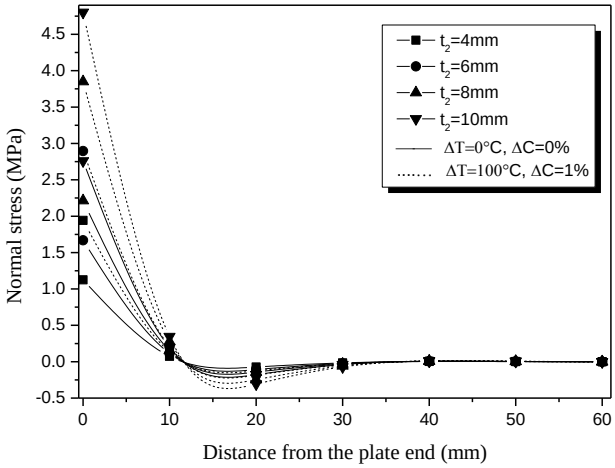

Fig.8 Effect of plate thickness on normal stress for an RC beam with a bonded composites laminates plate $[0/90]_s$ under hygrothermal effect.

4. Conclusion

The interfacial stresses of retrofitted RC beam strengthened with a soffit plate under hygrothermal and mechanical loads with taking into account the fibre volume fractions and orientation . The main conclusions found:

The hygrothermal effect increases considerably the maximum interfacial shear and normal stresses

the interfacial stresses increase with increasing the fibre volume fractions and with decreasing the angle of fibre orientation

The interfacial stresses increase with increasing the thickness of the FRP plate

Acknowledgements

The research described in this paper was supported by University of Sidi Bel Abbes and University center of Ain Temouchent in Algeria.

References

[1] Tounsi A, Benyoucef S., Int. J. Adhes. Adhes., (2007), 27: 207–215, doi:10.1016/j.ijadhadh.2006.01.009

[2] Tounsi A., Int. J. Solids. Struct., (2006), 43: 4154–4174, doi: 10.1016/j.ijsolstr.2005.03.074

[3] Benyoucef S, Tounsi A, Meftah S A and Adda Bedia EA., Compos. Interfaces., (2006), 13(7): 561–571, doi: 10.1163/156855406778440758

[4] Vilnay O., Int. J. Cem. Compos. Light. Weight. Concr., (1988), 10 (2): 73–78, doi: 10.1016/0262-5075(88)90033-4

[5] Roberts TM., (1989). *Approximate analysis of shear and normal stress concentrations in the adhesive layer of plated RC beams.* Struct. Eng. 1989, 67 (12): 229–233.

[6] Roberts TM, and Haji-Kazemi H. (1989). *Theoretical study of the behavior of reinforced concrete beams strengthened by externally bonded steel plates.* Proc. Inst. Civil. Eng., 87(2): 39–55

[7] Malek AM, Saadatmanesh H, and Ehsani MR.(1994). *Prediction of failure load of RC beams strengthened with FRP plate due to stress concentration at the plate end.* ACI. Struct. Journal., 95(1):142–152

[8] Robinovitch O. and Frostig Y. ,(200). *Closed-form higher-order analysis of beams strengthened with FRP strips.* J. Compos. Constr-ASCE, 4(2): 65–74

[9] Ye JQ. Cem. Concr. Compos. (2001). 23(4–5), 411–417, doi:10.1016/S0958-9465(01)00015-4

[10] Smith ST., and Teng JG., Eng. Struct. (2001). 23(7), 857–871, doi: 10.1016/S0141-0296(00)00090-0

[11] Barnes RA., and Mays GC., Int. J. Adhes. (2001). 21, 495–502, doi: 10.1016/S0143-7496(01)00031-8

[12] Stratford T., and Cadei J., Constr. Build. Mater. (2006). 20, 34–45, doi: 10.1016/j.conbuildmat.2005.06.041

[13] Bouazaoui Li A., Int. J. Adhes. (2008). 28, 101–108, doi: 10.1016/j.ijadhadh.2007.02.006

[14] Taljsten B., J. Mater. Civil. Eng. ASCE. (1997). 9(4), 206–12, doi: 10.1061/(ASCE)0899-1561(1997)9:4(206)

[15] Smith ST., and Teng JG., Eng. Struct. (2002). 24(4), 385–395, doi: 10.1016/S0141-0296(01)00105-5

[16] Smith ST., and Teng JG., Eng. Struct. (2002). 24(4), 397–417, doi: 10.1016/S0141-0296(01)00106-7

[17] Denton SN, (2001). Analysis of stresses developed in FRP plated beams due to thermal effects. FRP. Compos. In. civil. Eng., 527–536

[18] Smith ST., Teng JG., Eng Struct. (2001). 23(7), 857–871, doi: 10.1016/S0141-0296(00)00090-0

[19] Robinovitch O, and Frostig Y. (2001). Nonlinear higher-order analysis of cracked RCbeams strengthened with FRP strips. J. Struct. Eng- ASCE. 127(4): 381–389

[20] Shen HS., Teng JG., and Yang J., J. Eng. Mech. ASCE (2001). 127(4), 399–406, doi: 10.1061/(ASCE)0733-9399(2001)127:4(399)

[21] Hassaine Daouadji T. Advan. Comput. Design. (2017). 2(1), 57-69, doi: 10.12989/acd.2017.2.1.057

[22] Bouakaz K, Hassaine Daouadji T, Meftah SA, Ameur M, and Adda Bedia EA (2014). A numerical analysis of steel beams strengthened with composite materials. Mech. Compos. Mater. 50(4): 685-696

[23] Krour B, Bernard F, and Tounsi A. Eng. Struct. (2014). 56, 218-227, doi: 10.1016/j.engstruct.2013.05.008

[24] Touati M, Tounsi A, and Benguediab M. Comput. Concrete. (2015). 15(3), 141-166, doi: 10.12989/cac.2015.15.3.337

[25] Hadji L, Hassaine Daouadji T, Meziane AM, and Adda Bedia EA. Steel. Compos. Struct. Int. J. (2016). 20(2), 413-429, doi: 10.12989/scs.2016.20.2.413

[26] Kara IF. Struct. Eng. Mech. Int. J. (2016). 59(4), 775-793, doi: 10.12989/sem.2016.59.4.775

[27] Elamary AS, Abd-ELwahab RK. Struct. Eng. Mech. Int. J. (2016). 57(5), 937-949, doi: 10.12989/sem.2016.57.5.937

[28] Gibson R.F., (1994). Principles of composites material mechanics. McGraw-Hill Inc.

[29] Benkeddad. A, Grediac.M, Vautrin. A, (1995).On the transient hygroscopic stresses in laminated composite plates, composite Structures, Elsevier Applied Science, 30 (2), 201-205

[30] Benkeddad. A, Grediac.M, Vautrin. A, (1996). Computation of transient hygroscopic stresses in laminated composite plates, Composites Science and Technology, 56, 869-876

[31] Tounsi. A and Edda Bedia. E.A, (2003). Some observations on the evolution of transversal hygroscopic stresses in laminated composites plates: effect of anisotropy, Composite Structures, 59, 445-454

[32] Shen. C.H, (1981). Environmental effects in the elastic moduli of composite material. Environmental Effects on composite Materials, Springer.G.S, Ed, Technomic Publiching Company, 94-108.